Cyclic Transmembrane Charge Transport Mediated by Pyrylium and Thiopyrylium Ions

Rafail F. Khairutdinov and James K. Hurst*

Contribution from the Department of Chemistry, Washington State University, Pullman, Washington 99164-4630

Received January 2, 2001. Revised Manuscript Received May 25, 2001

Abstract: Transient spectroscopy revealed that 2,4,6-trimethylpyrylium, 2,4,6-triphenylpyrylium, and 2,4,6-triphenylthiopyrylium ions oxidatively quench excited triplet [5,10,15,20-tetrakis(4-sulfonatophenyl)porphinato]-zinc(II) to form the corresponding neutral radicals and the zinc porphyrin π-cation. The measured quenching rate constants were proportional to the pyrylium one-electron reduction potentials, that is, the reaction driving force. In the presence of anionic dihexadecyl phosphate vesicles, only the fraction of pyrylium not bound to the vesicle was capable of reacting with the photoexcited zinc porphyrin. Nonetheless, the pyrylium radicals mediated highly efficient transmembrane reduction of tris(2,2′-bipyridine)cobalt(III) contained within the inner aqueous core of the vesicles with apparent quantum yields that approached unity. Permeability coefficients (P) determined for the pyrylium radicals, pyrylium cations, and the proton were $10^{-4}-2 \times 10^{-5}$ cm/s, 10^{-10} cm/s, and $<5 \times 10^{-7}$ cm/s, respectively, so that only the neutral radicals are membrane-permeable on the time scale of the transmembrane redox reactions. However, each electron carrier was demonstrated to transport up to 200 electrons, at which point the internal pool of electron acceptors was exhausted. Since the cations are membrane-impermeable, a reaction cycle is proposed that includes hydrolysis of the pyrylium cations formed within the aqueous core to the corresponding 1,5-diketones which, as neutral molecules, can diffuse across the bilayer. According to this mechanism, while undergoing redox cycling the pyrylium ions function as cyclical antiporters of OH^- and the electron, thereby maintaining electroneutrality in the reaction compartments.

Introduction

Closed bilayer membranes have been effectively used as organizing matrixes for controlling reactivities of a wide variety of chemical and photochemical processes.[1−9] Many projected applications that rely on compartmentation of reaction components, for example, water photolysis or biomimetic photochemical syntheses,[10,11] require electroneutral carrier-mediated transmembrane redox steps in the overall reaction cycles. Nature makes widespread use of lipophilic quinones for this purpose, which vectorially cotransport protons and electrons as one arm of respiratory and photosynthetic redox loops that polarize energy-transducing membranes, driving coupled ATP synthesis and other forms of cellular work.[12] Quinones appear to suffer some disadvantages for applications outside living cells, however, including requiring a relatively large quinone "pool" within the membrane to obtain efficient charge transport,[10,11] chemical instability associated with formation of one-electron reduced hydroquinone radicals as initial redox products, and relatively slow transmembrane permeation rates.[13] We have correspondingly sought to identify alternative compounds that might function more effectively in artificial systems. In the present study, we have examined the capacity of pyrylium and thiopyrylium ions to act as combined quenchers of photoexcited redox dyes and transmembrane charge carriers to generate long-lived charge separation across bilayer membranes. By undergoing reversible ring-opening hydrolyses, these ions have the capacity to counter-transport electrons and OH^- ions, thereby effecting electroneutral vectorial transport of electronic charge. Furthermore, because both the one-electron reduced radicals and the ring-open oxidized forms are uncharged, rapid cyclic transmembrane diffusion of the carrier is possible. The pyrylium and thiopyrylium rings are chromophoric; direct photoexcitation led to efficient reductive quenching by electron acceptors. Thus, these ions can function as both photosensitizer and cyclic transmembrane charge carrier in vesicle-based integrated photochemical systems.

Experimental Section

Materials. Dithiothreitol ($D(SH)_2$), 2,4,6-triphenylpyrylium (TPP^+) tetrafluoroborate, 2,4,6-trimethylpyrylium (TMP^+) tetrafluoroborate, tetrasodium [5,10,15,20-tetrakis(4-sulfonatophenyl)porphinato]zinc(II)

* Address correspondence to this author. E-mail: hurst@wsu.edu. Telephone: (509) 335-7848. Fax: (509) 335-8867.

(1) Willner, I.; Willner, B. *Top. Curr. Chem.* **1991**, *58*, 153−218.
(2) Fendler, J. H. *Adv. Polym. Sci.* **1994**, *113*, 1−236.
(3) Bard, A. J. *Integrated Chemical Systems: A Chemical Approach to Nanotechnology*; New York: Wiley: 1994.
(4) Lehn, J. M. *Supramolecular Chemistry: Concepts and Perspectives*; VCH: Weinheim, 1995.
(5) Schneider, H.-J.; Yatsimirsky, A. K. *Principles and Methods in Supramolecular Chemistry*; John Wiley & Sons: New York, 2000.
(6) Kunitake T. *Supramolecular Chemistry of Biomimetic Systems*; John Wiley & Sons: New York, 2000.
(7) Hurst, J. K.; Khairutdinov, R. F. In *Electron Transfer in Chemistry*; Balzani, V., Ed.; Wiley-VCH: Weinheim, 2000; Vol. 4, pp 578−623.
(8) Hurst, J. K. In *Kinetics and Catalysis in Microheterogeneous Systems*; Gratzel, M., Kalyanasundaram, K., Eds.; Marcel Dekker: New York, 1991; pp 183−225.
(9) Lymar, S. V.; Hurst, J. K. *J. Phys. Chem.* **1994**, *98*, 989−996.
(10) Steinberg-Yfrach, G.; Liddell, P. A.; Hung, S.-C.; Moore, A. L.; Gust, D.; Moore, T. A. *Nature* **1997**, *385*, 239−241.
(11) Steinberg-Yfrach, G.; Rigaud, J.-L.; Durantini, E. N.; Moore, A. L.; Gust, T. A.; Moore, T. A. *Nature* **1998**, *392*, 479−482.
(12) Nicholls, D. G.; Ferguson, S. J. *Bioenergetics 2*; Academic Press: New York, 1992.
(13) Futami, A.; Hurt, E.; Hauska, G. *Biochim. Biophys. Acta* **1979**, *547*, 583−596.

10.1021/ja010017x CCC: $20.00
Published on Web 07/10/2001

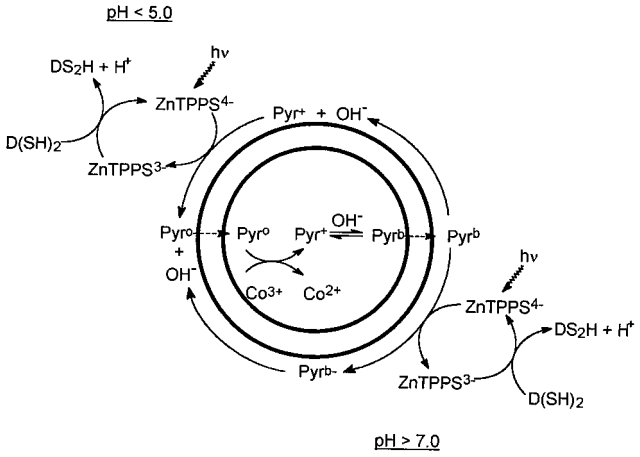

Figure 1. General reaction scheme for pyrylium-mediated photoinduced charge transfer. Two pathways are shown, one (upper half) initiated by oxidative quenching of the photosensitizer by the cation, Pyr^+, and the other (lower half) by the open-ring form, Pyr^b.

($ZnTPPS^{4-}$), and 6-carboxyfluorescein (CF) were best available grades from commercial suppliers and were used as received. 2,4,6-triphenylthiopyrylium ($TPTP^+$) tetrafluoroborate was prepared from 2,4,6-triphenylpyrylium tetrafluoroborate and sodium sulfide[14] and recrystallized from benzene. Tris(2,2′-bipyridine)cobalt(III) perchlorate was prepared as described[15] and recrystallized from water. All reagent solutions were prepared in Tris-Cl and/or acetate buffers using water purified with a Milli-Q system. Fresh stock solutions of $D(SH)_2$ were prepared prior to each set of experiments by dissolving weighed amounts of the free-flowing solid in buffer that had been deoxygenated by sparging with argon.

Small unilamellar dihexadecyl phosphate (DHP) vesicles, including those containing $Co(bpy)_3^{3+}$ in their inner aqueous phase, were prepared by sonication as described in detail elsewhere.[9,16] These suspensions were aged overnight at 4 °C to allow time for equilibration of protons in the internal and external aqueous phases. Pyrylium or thiopyrylium ions and/or $ZnTPPS^{4-}$ were subsequently added to the bulk external phase as required. The suspensions typically contained ∼4.4 mg/mL DHP, which corresponds to a vesicle concentration of ∼2 μM. Immediately prior to making photodynamic measurements, the suspensions were deoxygenated by bubbling with purified Ar, following which portions of $D(SH)_2$ reagent solutions were added anaerobically using syringe-transfer techniques. The complete system (Figure 1) was photoreactive and required protection from photodegradation by working in a minimal red light environment.

Photochemical Analyses. Continuous photolyses were performed using filtered light from a 1.5 kW xenon lamp as described previously;[17] notably, in experiments utilizing $ZnTPPS^{4-}$ as a photosensitizer, a 420 nm interference filter was used to limit illumination to the Soret band. Reduction of $Co(bpy)_3^{3+}$ was monitored spectrophotometrically at 320 nm using $\epsilon_{320} = 2.85 \times 10^4\ M^{-1}\ cm^{-1}$ for the $Co(bpy)_3^{3+} - Co(bpy)_3^{2+}$ difference extinction coefficient.[9] Absolute quantum yields were measured at a light intensity of 6×10^{-9} einstein/s, determined using a calibrated bolometer. Absorption spectra and formation and decay kinetics of reaction intermediates were measured by laser flash photolysis using the second (532 nm) or third (355 nm) harmonic output from a Continuum Surelite III Nd:YAG laser as the excitation source. The explicit procedures and instrumental setup used for the transient-kinetic studies are described in detail elsewhere.[17]

Hydrolysis of Pyrylium and Thiopyrylium Ions. Ring-opening hydrolysis rates and equilibria of these ions were determined spectrophotometrically by using a Hewlett-Packard 8452 diode array spectrophotometer interfaced to a Chemstation data acquisition/analysis system. The following parameters were used to record and analyze the data: in aqueous solutions, TMP^+, 287 nm ($\epsilon = 1.5 \times 10^4\ M^{-1}\ cm^{-1}$); TPP^+, 355 nm ($\epsilon = 3.9 \times 10^4\ M^{-1}\ cm^{-1}$); $TPTP^+$, 372 nm ($\epsilon = 2.6 \times 10^4\ M^{-1}\ cm^{-1}$); in DHP vesicle suspensions, TMP^+, 287 nm ($\epsilon = 1.5 \times 10^4\ M^{-1}\ cm^{-1}$); TPP^+, 366 nm ($\epsilon = 5.4 \times 10^4\ M^{-1}\ cm^{-1}$); $TPTP^+$, 386 nm ($\epsilon = 3.5 \times 10^4\ M^{-1}\ cm^{-1}$). Typically, reactions were initiated by adding ∼100 μL of 0.1 N NaOH in 40 mM acetate to a 1 cm optical cuvette containing ∼ 1×10^{-5} M pyrylium or thiopyrylium salt in 2.4 mL 40 mM acetate buffer, pH 5.0, with or without DHP. This amount of base increased the alkalinity to pH 11. In cycling experiments, the initial pH was subsequently restored by adding ∼100 μL of 0.1 N HCl in 40 mM acetate buffer. Equilibrium constants for the pH-dependent ring-opening−closing reaction (Scheme 1) were determined from the optical spectra recorded over the range of pH 2−10. Several isosbestic points were observed for each of the pH titrations (see, e.g., the inset to Figure 5); consequently, the data were treated as simple two-species equilibria.

Scheme 1

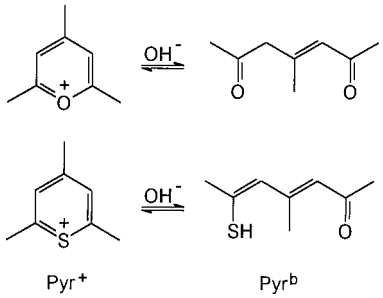

Membrane Binding and Dynamics. The extents of binding of $ZnTPPS^{4-}$, $Co(bpy)_3^{3+}$, and pyrylium and thiopyrylium ions to DHP vesicles were determined by membrane ultrafiltration using 30,000 MW cutoff (Centricon-30) centrifugal microconcentrators.[17] Transmembrane permeation of TPP^+ and $TPTP^+$ was estimated by occluding these ions within the vesicles and following their rates of leakage into the external medium. For these experiments, DHP vesicles were formed in 40 mM acetate buffer, pH 5.0, containing ∼4×10^{-5} M of TPP^+ or $TPTP^+$, followed by removal of extravesicular pyrylium or thiopyrylium ions by passing the suspension down a 0.7 cm × 8 cm Bio-Rad AG 50W-X8 cation exchange column. The vesicle suspensions were then rechromatographed at timed intervals, and the corresponding losses of TPP^+ or $TPTP^+$ in the vesicle-containing effluent fractions were determined spectrophotometrically. Quantitative removal of TPP^+ and $TPTP^+$ from the external vesicle surface was confirmed by probing for hydrolysis following increasing the external pH to 11. At this pH, hydrolysis of these ions is complete within ∼80 s. However, no spectral changes were observed within 100 s following the pH jump, indicating that all of the TPP^+ or $TPTP^+$ that coeluted with the vesicles was confined to the vesicle interior. These techniques could not be used to measure transmembrane diffusion of TMP^+ because only very small amounts of this ion were entrapped within the vesicles.

To measure the proton permeability through the DHP bilayer, DHP vesicles containing entrapped 6-carboxyfluorescein were prepared by sonication in 20 mM Tris buffer, pH 7−8, containing ∼10^{-4} M CF. Most of the extravesicular CF was then removed by passage down a 0.7 cm × 8 cm anion-exchange column (Bio-Rad AG 1-X8, chloride form, 100−200 mesh) that had been equilibrated with buffer. The CF-loaded vesicles were placed in a fluorescence cuvette and acidified by adding an appropriate amount of 20 mM Tris buffer, pH 1.3. Subsequent changes in the internal pH were monitored by following the decay in fluorescence emission intensity at 514 nm (λ_{ex} = 492 nm). The measured fluorescence intensities were then scaled to that of the extravesicular pH by adding 100 μL of Triton X-100, which collapsed the transmembrane pH gradient by permeabilizing the membranes. Subsequent comparison to an I_{514} versus pH calibration curve allowed estimation of the internal pH of the vesicles at any time following the pH jump.

(14) Wizinger, R.; Ulrich, P. *Helv. Chim. Acta* **1956**, *39*, 207−216.
(15) Burstall, F. H.; Nyholm, R. S. *J. Chem. Soc.* **1952**, 3570−3579.
(16) Humphry-Baker, R.; Thompson, D. H.; Lei, Y.; Hope, M. J.; Hurst, J. K. *Langmuir* **1991**, *7*, 2592−2601.
(17) Lymar, S. V.; Khairutdinov, R. F.; Soldatenkova, V. A.; Hurst, J. K. *J. Phys. Chem.* **1998**, *102*, 2811−2819.

Table 1. Fractions of Unbound Pyrylium and Thiopyrylium Ions (f), Rate Constants for Oxidative Quenching $(k_q)_v$,[a] and Quantum Yields for $Co(bpy)_3^{3+}$ Reduction to $Co(bpy)_3^{2+}$ (ϕ)[b]

[OAc$^-$] (mM)	f_{TPP^+} (±30%)	f_{TPTP^+} (±30%)	$(k_q^{TPP^+})_v$ (10^7 M^{-1} s^{-1})	$(k_q^{TPTP^+})_v$ (10^7 M^{-1} s^{-1})	ϕ_{TPP^+} (±30%)	ϕ_{TPTP^+} (±30%)
20	0.01	0.015	3(3.5)	2(2.3)	0.07	0.06
30	0.02	0.025	5(7)	3(3.8)	0.1	0.1
50	0.025	0.032	7(8.7)	5(4.9)	0.15	0.12
70	0.04	0.05	11(14)	9(7.7)	0.2	0.2
100	0.06	0.07	14(21)	10(11)	0.25	0.2

[a] Values given in parentheses are calculated from the expression $(k_q)_v = fk_q$. [b] At pH 5.0, 22 °C, with $[Pyr^+] = 1.5$ μM and $[D(SH)_2] = 500$ μM.

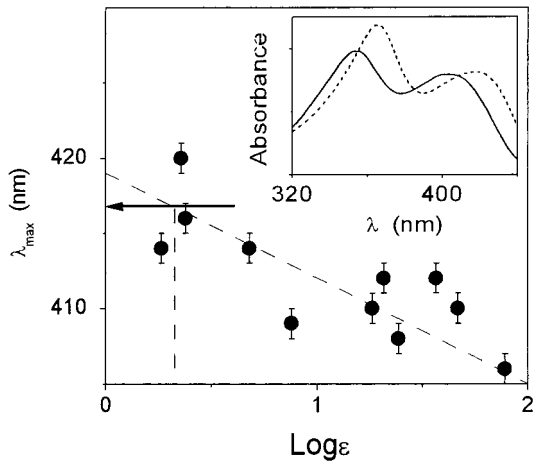

Figure 2. Solvent dependence of the low-energy band maximum for TPP^+. The solvents used (with ϵ in parentheses)[47] were pentane (1.84), benzene (2.28), toluene (2.38), $CHCl_3$ (4.8), tetrahydrofuran (7.6), 2-propanol (18.3), 1-propanol (20.1), ethanol (24.3), dimethyl sulfoxide (46.7), and water (78). The arrow shows the position of the absorption band for DHP vesicle-bound TPP^+, which corresponds to an apparent ϵ of ~2. The inset gives the absorption spectrum in 40 mM acetate, pH 5.0, in the absence (solid line) and presence (dashed line) of DHP vesicles, $[TPP^+] = 10$ μM.

Results and Discussion

Topographic Organization of the System. Partitioning of reaction components between membranous and aqueous phases can strongly influence the photoreaction dynamics of vesicle-organized systems.[7] This partitioning can be conveniently measured by membrane ultrafiltration,[17] which was used to determine the extent of TPP^+ and $TPTP^+$ binding to the anionic DHP vesicles under our experimental conditions. Specifically, by equating the experimentally measured effluent concentration of the pyrylium or thiopyrylium ions in the ultrafiltration experiment with the concentration of unbound ions in the presence of vesicles, the fraction (f) of free TPP^+ and $TPTP^+$ can be calculated from $f = [Pyr^+]_f/([Pyr^+]_f + [Pyr^+]_b)$; in this equation, the subscripts b and f refer to membrane-bound and unbound species, respectively, and the sum, $[Pyr^+]_b + [Pyr^+]_f$, is the total added pyrylium or thiopyrylium ions. The results, listed in Table 1, indicate that binding for both TPP^+ and $TPTP^+$ was >90% under all experimental conditions. Nonetheless, the extent of binding increased with decreasing buffer concentration in the medium, suggesting that electrostatic attractive forces between the anionic DHP membrane interface and the cations contributed to the binding interactions. The lowest-energy absorption bands of TPP^+ and $TPTP^+$ exhibited bathochromic shifts of ~10 nm upon binding to the vesicles (Figure 2, insert). These bands also exhibited shifts of up to 15 nm upon transfer from water to low-polarity solvents (Figure 2), indicating that the bound ions were localized to a relatively nonpolar environment within the headgroup region of the membrane,[18] and therefore that hydrophobic interactions also contribute to the strong association to the vesicle membrane. Membrane ultrafiltration studies established that binding of TMP^+ and the anions $ZnTPPS^{4-}$ and CF to the anionic vesicles was negligible, although binding of $Co(bpy)_3^{3+}$ was >90%, as had been found in earlier work.[17] Consistent with this result, no spectral changes were observed when DHP vesicles were added to aqueous solutions of TMP^+, although its near-ultraviolet band was red-shifted in nonpolar solvents.

Transmembrane Diffusion Dynamics. The experiments described in this section were undertaken to verify that the intrinsic permeabilities of H^+ and the pyrylium cations across DHP membranes are too low relative to the neutral forms of the redox carriers to allow their participation in the transmembrane redox reaction. In general, among simple cations the proton exhibits an exceptionally high permeability coefficient through hydrocarbon bilayers;[19] consequently, one can safely assume that passive transmembrane diffusion of other electrolyte cations does not occur if the proton is found to be impermeable. Furthermore, electrolyte anion transport will be severely hindered by the strong repulsive potential at the aqueous−organic interface that is generated by the anionic DHP phosphate headgroups.

Proton Permeability. Proton permeabilities (P_{H^+}) have been determined in a variety of ways for planar lipid bilayers and liposomes constructed from phospholipid membranes. Reported values for P_{H^+} range over 5 orders of magnitude, from $\sim 10^{-7}$ to $\sim 10^{-2}$ cm/s, and depend on the bilayer systems used, their lipid composition and hydrocarbon chain length, the supporting medium, and the experimental techniques used.[19] Values for DHP vesicles have not been previously measured, in part because the phosphate headgroup is highly buffering in the neutral pH region and the vesicles are exceptionally small,[16] making it difficult to measure internal pH changes. Nonetheless, the value for DHP vesicles is expected to lie at the lower limit for liposomes since the DHP membrane is in its relatively viscous gel phase,[16] whereas the liposomes are usually in their fluid, or liquid crystalline, phase at ambient temperatures.

Diffusion of H^+ across the DHP bilayer membrane was investigated by monitoring the decrease in fluorescence intensity following acidification of suspensions of vesicles containing 6-carboxyfluorescein entrapped within their aqueous cores.[20] A typical result, describing the temporal response to a jump in acidity in the external medium, is given in Figure 3. The initial rapid phase, which is instantaneous on the observational time scale, is attributed primarily to protonation of the fraction of the probe that was located in the external aqueous phase, with a minor contribution arising from dilution of the solution. The amplitude of this portion could be decreased, but not completely removed, by repetitive passage of the vesicle suspension down an anion exchange column. The amount shown in Figure 3 represents about 1% of the CF originally present in the external solution when the vesicles were formed. Addition of the detergent, Triton X-100, also led to discontinuous, nearly complete quenching of fluorescence (Figure 3), consistent with rapid equilibration of the aqueous compartments accompanying disruption of the bilayer structure. The slow, relatively small

(18) Khairutdinov, R. F.; Giertz, K.; Hurst, J. K.; Voloshina, E. N.; Voloshin, N. A.; Minkin, V. I. *J. Am. Chem. Soc.* **1998**, *120*, 1270−12713.
(19) Paula, S.; Volkov, A. G.; Van Hoek, A. N.; Haines, T. H.; Deamer, D. W. *Biophys. J.* **1996**, *70*, 339−348.
(20) See, e.g.: Zeng, J.; Smith, K. E.; Chong, P. L.-G. *Biophys. J.* **1993**, *65*, 1404−1414 and references therein.

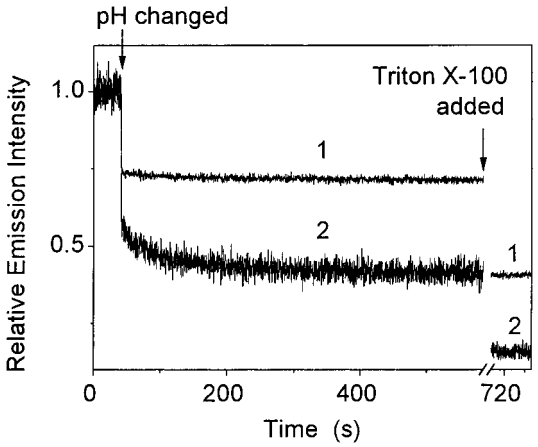

Figure 3. Kinetics of loss in emission intensity of 6-carboxyfluorescein-loaded DHP vesicles upon acidification of the medium. Overall changes accompanying jumps from 7.5 to 5.8 (trace 1) and 7.0 to 5.0 (trace 2); $\lambda_{ex} = 492$ nm, $\lambda_{em} = 514$ nm.

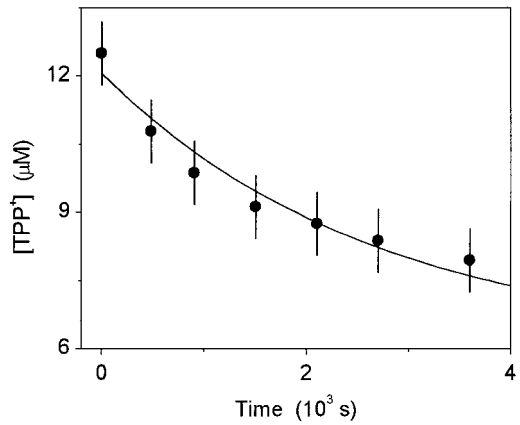

Figure 4. Temporal loss of TPP^+ occluded within the aqueous core of DHP vesicles. Closed circles are experimental data; the solid curve is the fit of the data to eq 1 using $\tau = 5 \times 10^3$ s. Reaction conditions are described in the text.

decrease in fluorescence following the rapid initial drop (Figure 3) has the characteristics expected for transmembrane permeation of H^+ or OH^- ions across the bilayer. Specifically, the rate is quickly attenuated and stops well before the pH reported by the dye reaches equilibrium with the bulk solution (Figure 3). Such behavior is expected if transmembrane diffusion of H^+ or OH^- ions down their concentration gradients were not matched by charge-compensating diffusion of other ions in the system. Under these circumstances, a transmembrane potential will develop that opposes further diffusion of H^+ or OH^-.[21] Quantitative analysis of the relaxation dynamics indicates that additional processes contribute to the fluorescence changes, however.[22] Thus, only an upper limit for proton diffusion of $P_{H^+} < 5 \times 10^{-7}$ cm/s can be set from the data.[23]

Permeabilities of TPP^+ and $TPTP^+$. Measurement of the rates of diffusion of these DHP-associated ions was initiated by removing the externally bound component by cation-exchange chromatography, then repeating the chromatographic step on portions of the vesicle suspension at timed intervals. As illustrated in Figure 4, the amount of dopant ion removed on the second pass was proportionately greater the longer the time interval between the chromatographic steps, indicating that diffusion of the pyrylium or thiopyrylium ions from the membrane internal surface to the external surface was occurring on the same time scale. Because the time scales for transmembrane diffusion of TPP^+ and $TPTP^+$ are considerably longer than that for the proton (cf. Figures 3 and 4), transmembrane potentials generated by their electrogenic diffusion should be dissipated by charge-compensating diffusion of H^+ in these buffered environments. In this case, since these ions are strongly adsorbed to the DHP vesicles, the rate law describing net outward diffusion can be approximated as $dn_i/dt = (n_o - n_i)/\tau$, where n_i and n_o are the number of TPP^+ or $TPTP^+$ ions adsorbed on the internal (i) or external (o) vesicle surface and $\tau = 1/k_D$ is the characteristic time for transmembrane diffusion. In this model, the first-order rate constants (k_D) for inward and outward diffusion are assumed to be identical. Given the additional constraints that the external concentration of ions at the start of the reaction is zero, and that the total amount of ions (n_T) is constant, $n_i + n_o = n_T$, one obtains upon integration of the rate law:

$$n_i = \frac{n_T}{2}\left(\exp\left(-\frac{2t}{\tau}\right) + 1\right) \quad (1)$$

Application of eq 1 to the experimental data gave a best-fit value for TPP^+ of $\tau = 5\ (\pm 1) \times 10^3$ s (Figure 4, solid line) and for $TPTP^+$ of $\tau = 8\ (\pm 2) \times 10^3$ s. Corresponding values for the permeability coefficients, calculated from $P = d/\tau$ where $d = 4 \times 10^{-7}$ cm is the bilayer width,[16] were $P_{TPP^+} = 8 \times 10^{-11}$ cm/s and $P_{TPTP^+} = 5 \times 10^{-11}$ cm/s. Collectively, the low values measured for P_{H^+}, P_{TPP^+}, and P_{TPTP^+} indicate that there is a relatively high energetic barrier to diffusion across the bilayer. This barrier may have its origins in the tight hydrocarbon chain packing in the lipid core of the DHP membrane.[16] In any event, the physical and diffusional properties of TPP^+ and $TPTP^+$ suggest that they are trapped within relatively deep energetic wells located within the hydrocarbon phase near the aqueous−organic interfaces. This description is consistent with conventional models describing the binding of lipophilic ions to membranes.[18,24−26]

Ring-Opening Hydrolyses of Pyrylium and Thiopyrylium Ions. Pyrylium and thiopyrylium ions undergo reversible addition of hydroxide ion in aqueous media to form uncharged 1,5-diketones[27] and 1,5-thioglutaconic aldehydes,[28] respectively (Scheme 1); this reaction can be described by the equilibrium, $Pyr^+ + H_2O \rightleftharpoons Pyr^b + H^+$, which defines an acid dissociation constant (K_a).

Formation of the pseudobase Pyr^b is accompanied by loss of the prominent Pyr^+ near-UV optical bands (Figure 5 inset), as

(21) Evans, D. F.; Wennerstrom, H. *The Colloidal Domain*; Wiley-VCH: New York, 1999.

(22) From the lower trace in Figure 3, the internal pH is calculated to change from pH 7.0 to 6.7, corresponding to an apparent uptake of ~80 H^+ ions per vesicle. If uncompensated, this would generate a $\Delta\Psi$ of ~1 V.[8] However, the maximal $\Delta\Psi$ that the imposed pH gradient can generate is only 120 mV.

(23) Immediately after the external pH jump, $\Delta\Psi = 0$. In this case,[21] $P_{H^+} = B_i V_i / S(dpH_i/dt)_0([H^+]_0 - [H^+]_i^0)^{-1}$ where S and V_i are the surface area and internal volume of the vesicle, B_i is the internal buffering capacity, $[H^+]_0 - [H^+]_i^0$ is the imposed proton gradient, and $[dpH_i/dt]_0$ is the experimentally determined rate of change in internal pH. B_i was estimated from pH titration curves of DHP vesicle suspensions to be 3×10^{-3} M. Using this value and previously determined S and V_i,[16] one calculates an apparent $P_{H^+} = 5 \times 10^{-7}$ cm/s.

(24) Anderson, O. S.; Fuchs, M. *Biophys. J.* **1975**, *15*, 795−830.

(25) Ketterer, B.; Neumke, B.; Lauger, P. *J. Membr. Biol.* **1971**, *5*, 225−245.

(26) Kachel, K.; Asuncion-Punzalan, E.; London, E. *Biochim. Biophys. Acta* **1998**, *1374*, 63−76.

(27) Berson, J. A. *J. Am. Chem. Soc.* **1952**, *74*, 358−360.

(28) Doddi, G.; Ercolani, G. *Adv. Heterocycl. Chem.* **1994**, *60*, 66−195.

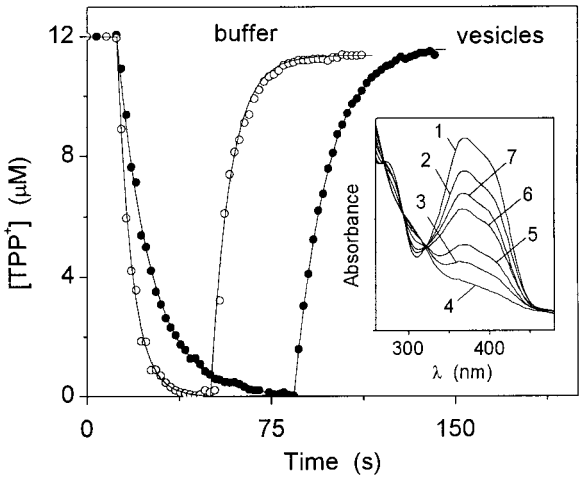

Figure 5. Kinetics of $TPTP^+$ hydrolysis monitored by changes in absorption at 390 nm. Open circles: 12 μM $TPTP^+$ in 40 mM acetate, pH 5.0; closed circles: an identical solution containing ~2 μM DHP vesicles. At 12 s, the pH was jumped from 5.0 to 11.0; at 50 s (open circles) and 84 s (closed circles), the original pH was restored. The solid lines are data fits to exponential rate laws with $\tau = 6$ s (buffer) and 13.5 s (vesicles). The inset shows the changes in optical spectra for the homogeneous reaction at various times, specifically: $t = 12$ s (1); 14 s (2); 22 s (3); 50 s (4); 64 s (5); 66 s (6); 74 s (7).

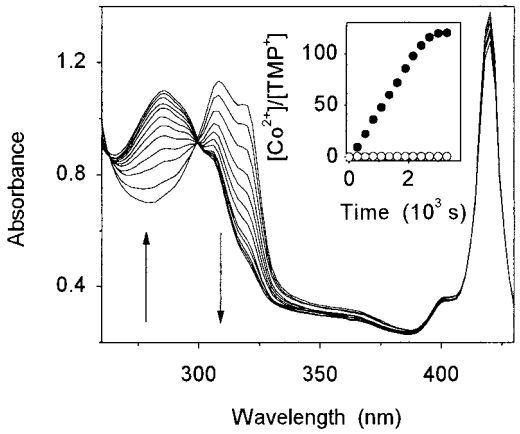

Figure 6. Optical spectral changes accompanying illumination of the complete system (Figure 1). Conditions: $[TMP^+] = 1$ μM; $[D(SH)_2] = 1$mM; $[ZnTPPS^{4-}] = 12.5$ μM; $[Co(bpy)_3^{3+}] = 120$ μM; with the aqueous vesicle core containing 20 mM Tris, pH 8.0, and the bulk solution containing 10 mM Tris plus 20 mM acetate, pH 5.0. The near-UV trough-and-peak structure and isosbestic points are indicative of $Co(bpy)_3^{3+}$ to $Co(bpy)_3^{2+}$ reduction.[9] The kinetics of $Co(bpy)_3^{2+}$ accumulation in the presence (closed circles) and absence of TMP^+ (open circles) are shown in the inset.

well as small changes in the ultraviolet region and the appearance of a new low-intensity band in the visible region. Spectrophotometrically determined values of K_a measured under our reaction conditions were 8.3×10^{-6} M for TMP^+, 2.5×10^{-5} M for TPP^+, and 5.0×10^{-7} M for $TPTP^+$; these values lie within the range typically found for this type of equilibrium ($K_a = 10^{-5}$–10^{-7} M).[28,29]

The kinetics of hydrolysis of TMP^+, TPP^+, and $TPTP^+$ in aqueous solutions obeyed first-order rate laws whose constants increased linearly with $[OH^-]$ in the alkaline region. The ring-opening reactions of TMP^+ were uninfluenced by addition of DHP vesicles, consistent with negligible interaction with the membrane interface. However, the reactions of TPP^+ and $TPTP^+$ were retarded ~2-fold in the presence of the vesicles (Figure 5) and, at dopant levels above ~30 ions/vesicle, exhibited pronounced biphasic kinetics (Figure S1, Supporting Information). The dependence upon pyrylium mole fraction suggests partial aggregation or lateral phase separation within the membrane bilayer, with the aggregated form undergoing much slower ring opening. For these experiments, TPP^+ and $TPTP^+$ were added to preformed vesicles immediately prior to jumping the medium pH; consequently, the alternative possibility that the fast and slow phases reflect ring-opening reactions of the ions located at the outer and inner vesicle interfaces, respectively, can be excluded because they did not have sufficient time to diffuse across the bilayer. Fluorescence spectroscopy provided direct evidence of aggregation of DHP-bound $TPTP^+$ (Figure S2, Supporting Information). Excitation at 400 nm of a suspension containing 20 $TPTP^+$/vesicle gave an emission band at 499 nm, which was very similar in intensity and emission maximum (486 nm) for the free ion in solution, whereas an identical amount of $TPTP^+$ at a dopant level of 160 $TPTP^+$/vesicle gave a band with markedly red shifted emission maximum (534 nm) whose intensity was quenched by ~50%. In contrast, the fluorescence intensities and band shapes of DHP-bound TPP^+ were very similar to that of free TPP^+ at dopant levels as high as 200 TPP^+/vesicle.

The negative charge on the DHP vesicle surface attracts protons, causing the interface to be more acidic than the bulk solution.[30] This effect should reduce the rate of pseudobase formation by the bound TPP^+ and $TPTP^+$ ions. Assuming a surface potential of $\Psi_S \approx -0.15$ V,[31] one estimates from the equation, $pH_m - pH_b = -F\Psi_S/2.3RT$ that, at the membrane interface, $pH_m \approx 8$ when that of the bulk solution is $pH_b = 10.6$. If the apparent interfacial pH were the only effect controlling reactivity, one would expect from the pH dependence of the reaction in solution a hydrolysis rate ~400-fold slower for the bound ions. The much smaller difference in rate (~2-fold) suggests that ring-opening hydrolysis is promoted by the nonpolar environment of the membrane binding site. Thus, at equivalent pH values, hydrolysis of the bound ions would be ~10^2-fold greater than the free ions in aqueous solution.

Continuous Photolysis. Continuous illumination of the complete system (Figure 1) containing $Co(bpy)_3^{3+}$ in the internal aqueous phase and $ZnTPPS^{4-}$ pyrylium or thiopyrylium ions (TPP^+, $TPTP^+$, or TMP^+), and an electron donor ($D(SH)_2$) in the external aqueous solution gave rise to net reduction of the occluded $Co(bpy)_3^{3+}$ to $Co(bpy)_3^{2+}$ (Figure 6). The kinetics of $Co(bpy)_3^{2+}$ accumulation in the presence of TMP^+ monitored at 320 nm is given in the inset in Figure 6. For all three Pyr^+ ions, photoreduction of $Co(bpy)_3^{3+}$ required that all reaction components be present. This behavior is qualitatively similar to that observed earlier in similar assemblies that utilized *N*-alkyl-4-cyanopyridinium cations (C_nCP^+) in place of the Pyr^+ ions as redox quenchers.[17] In those systems, net photoinduced one-electron reduction of C_nCP^+ was followed by transmembrane diffusion of C_nCP^o and reduction of $Co(bpy)_3^{3+}$ in the internal aqueous phase. A quantitative difference between these two systems is the relative amount of $Co(bpy)_3^{3+}$ ions reduced per quencher/mediator molecule. Because the C_nCP^+ ions are membrane-impermeable, reoxidation following transmembrane diffusion of C_nCP^o led to efficient entrapment within the vesicle. Consequently, only one $Co(bpy)_3^{3+}$ could be reduced per C_n-

(29) Williams, A. *J. Am. Chem. Soc.* **1971**, *93*, 2733−2737.

(30) Gennis, R. B. *Biomembranes. Molecular Structure and Function*; Springer-Verlag: New York, 1989.

(31) Drummond, C. J.; Greiser, F. *Photochem. Photobiol.* **1987**, *45*, 19−34.

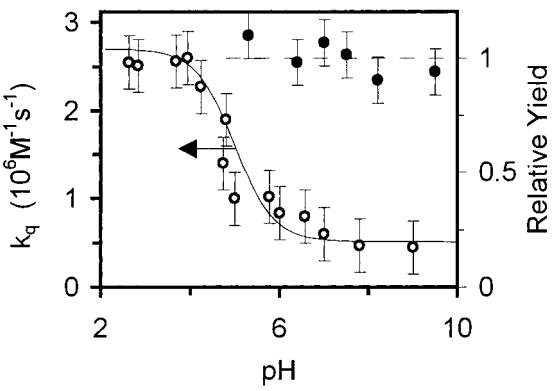

Figure 7. pH-dependencies of the triplet-photoexcited ZnTPPS^{4-} quenching rate constant (k_q) by TMP$^+$(open circles) and the relative yields of Co(bpy)$_3^{3+}$ to Co(bpy)$_3^{2+}$ reduction (closed circles). Conditions: [TMP$^+$] = 150 μM, [D(SH)$_2$] = 1mM, [ZnTPPS^{4-}] = 12.5 μM, [Co(bpy)$_3^{3+}$] = 47 μM, in 20 mM acetate buffer. The solid line represents the best fit of the experimental data by eq 3 using $k_q^1 = 2.7 \times 10^6$ M^{-1} s^{-1}, $k_q^2 = 5.1 \times 10^5$ M^{-1} s^{-1}, and $K_a = 8.3 \times 10^{-6}$ M.

CP$^+$ ion added to the bulk medium. For the data presented in Figure 6, the amount of Co(bpy)$_3^{2+}$ formed exceeded the total amount of added TMP$^+$ by 120-fold, implying that TMP$^+$ was capable of functioning as a cyclical transmembrane electron carrier (Figure 1).[32] The maximal number of redox cycles that could be demonstrated in these systems was limited by the amount of Co(bpy)$_3^{3+}$ that could be entrapped within the vesicles to ~200. Under the experimental conditions, ZnTPPS^{4-} and TMP$^+$ were photostable, but TPP$^+$ and TPTP$^+$ underwent slow photobleaching with a quantum yield of $\sim 5 \times 10^{-5}$. Net photoreduction of Co(bpy)$_3^{3+}$ also occurred when the ZnTPPS^{4-} Q-bands were illuminated; by exciting with visible light, photodestruction of TPP$^+$ and TPTP$^+$ could be avoided. The possibility that compartmentation of the photosensitizer or electron acceptor (Figure 1) might be lost upon exposure to the photolyzing light source was examined by column chromatography of the product solutions; these analyses gave no evidence for incorporation of ZnTPPS^{4-} within or of Co(bpy)$_3^{3+}$ release from the inner aqueous phase of the vesicles. Slow release of the Co(bpy)$_3^{2+}$ product ion ($k \cong 1 \times 10^{-4}$ s^{-1}) was detected using column chromatographic procedures analogous to those described for studying pyrylium ion permeation of the bilayer.[33]

The net quantum yields for Co(bpy)$_3^{3+}$ reduction (ϕ) in systems containing TPP$^+$, TMP$^+$, or TPTP$^+$ were dependent upon the concentrations of system components and medium conditions. Specifically, they: (1) were pH-independent in weakly acidic to weakly basic media (Figure 7), (2) increased with increasing ionic strength of the medium (Table 1), (3) increased with concentration of the redox mediator, and (4) increased with concentration of electron donor at [D(SH)$_2$] $\leq$ 400 μM, but were constant at higher donor concentrations. Representative values for ϕ are given in Table 1.

Transient Kinetics. Reactions of ^{3}ZnTPPS^{4-} with Pyrylium and Thiopyrylium Ions. Electron transfer from ^{3}ZnTPPS^{4-} to Pyr$^+$ is exergonic ($E°$ (ZnTPPS^{3-}/^{3}ZnTPPS^{4-}) = -0.75 V;[34] $E°$ (TPP$^{+/o}$) = -0.13 V;[35] $E°$ (TPTP$^{+/o}$) = 0.03 V;[35,36] $E°$ (TMP$^{+/o}$) = -0.44 V;[35] all potentials vs NHE). In both aqueous solutions and DHP vesicle suspensions, addition of TPP$^+$, TPTP$^+$, or TMP$^+$ caused the ^{3}ZnTPPS^{4-} decay rate to increase. Transient spectroscopy revealed intermediary formation of the ZnTPPS^{3-} π-cation radical,[37] i.e., the reaction involved oxidative quenching of the photoexcited triplet by Pyr$^+$:

$$^3\text{ZnTPPS}^{4-} + \text{Pyr}^+ \xrightarrow{k_q^1} \text{ZnTPPS}^{3-} + \text{Pyr}^o \qquad (2)$$

In the absence of electron donors, back-electron transfer between the photoproducts to regenerate ZnTPPS^{4-} and Py$^+$ was apparently highly efficient since no changes were observed in the transient and ground-state absorption spectra or in the decay rate of ^{3}ZnTPPS^{4-} following excitation by more than 100 laser pulses. The quenching rate constants (k_q^1) in 20 mM acetate buffer, pH 5.0, measured from the dependence of the pseudo-first-order decay upon the oxidant concentrations, increased with the reaction driving force; specifically, for TPP$^+$, TPTP$^+$, and TMP$^+$, $k_q^1 = 3.5 (\pm 0.7) \times 10^9$ M^{-1} s^{-1}, 2.3 ($\pm$0.5) $\times 10^9$ M^{-1} s^{-1}, and 2.7 ($\pm$0.5) $\times 10^6$ M^{-1} s^{-1}, respectively. As illustrated for TMP$^+$ in Figure 7, these rate constants decreased with increasing pH over the same regions where ring-opening hydrolysis of the Pyr$^+$ ions occurred, but did not fall to zero at higher alkalinities. This behavior suggests that Pyr^b can also oxidatively quench ^{3}ZnTPPS^{4-}, albeit less efficiently. The quenching rate constant for the diketone (k_q^2) was determined by fitting the pH-dependent experimental quenching constant (k_q) to the following equation:

$$k_q = \frac{k_q^1}{1 + 10^{\text{pH}-\text{p}K_a}} + \frac{k_q^2 \times 10^{\text{pH}-\text{p}K_a}}{1 + 10^{\text{pH}-\text{p}K_a}} \qquad (3)$$

using the independently determined values for K_a and k_q^1. The best-fit value for k_q^2 (5 ($\pm$2) $\times 10^5$ M^{-1} s^{-1}) is shown as the solid line in Figure 7; corresponding values for TPP$^+$ and TPTP$^+$ are 1.1 ($\pm$0.3) $\times 10^8$ M^{-1} s^{-1} and 9 ($\pm$3) $\times 10^7$ M^{-1} s^{-1}, respectively.

The pH-independent yields for transmembrane reduction of Co(bpy)$_3^{3+}$ under these conditions (Figure 7) indicate that both Pyr$^+$ and Pyr^b can efficiently transport electrons across the anionic DHP membrane. However, one-electron reduction of the neutral diketones would generate radical anions whose permeabilities, and hence efficiencies for reducing entrapped Co(bpy)$_3^{3+}$, should be much less than neutral molecules. Presumably, these radical anions undergo ring closure to form neutral pyrylium and thiopyrylium radicals before traversing the bilayer (Figure 1, lower pathway).

The efficiency of reaction 2 was not altered by addition of DHP vesicles when TMP$^+$ was the oxidant, whereas quenching by TPP$^+$ and TPTP$^+$ was markedly attenuated when DHP vesicles were present in the medium. This effect is illustrated in Figure 8. In vesicular suspensions, the apparent quenching rate constant $(k_q)_v$ for TPP$^+$ and TPTP$^+$ was about 2 orders of magnitude less than in homogeneous solution and increased with the medium ionic strength (Table 1). This pattern of reactivity indicates that the vesicle-bound ions were markedly less reactive toward ^{3}ZnTPPS^{4-} than free TPP$^+$ and TPTP$^+$. In this case, the apparent rate constant obeyed the relationship, $(k_q)_v \cong f k_q$ (Table 1).[13]

The portion of ^{3}ZnTPPS^{4-} undergoing oxidative quenching by TPP$^+$ and TPTP$^+$ (ϕ_1) is given by the equation, $\phi_1 = (k_q)_v[\text{Pyr}^+]\tau_o/1 + \{1 + (k_q)_v[\text{Pyr}^+]\tau_o\}$, where $\tau_o = 2.1$ ms is the intrinsic lifetime of ^{3}ZnTPPS^{4-}.[17] The yield of photogenerated Pyr^o radicals that undergo transmembrane electron transport (ϕ_t)

(32) Khairutdinov, R. F.; Hurst, J. K. *Nature* **1999**, *402*, 509−511.
(33) Khairutdinov, R. F.; Hurst, J. K. *Langmuir*. Manuscript submitted.
(34) Kalyanasundaram, K.; Neumann-Spallart, M. *J. Phys. Chem.* **1982**, *86*, 5163−5174.
(35) Wingens, V.; Pouliquen, J.; Kossanyi, J.; Heintz, M. *New J. Chem.* **1986**, *10*, 345−350.
(36) Saeva, F. D.; Olin, G. R. *J. Am. Chem. Soc.* **1980**, *102*, 299−303.
(37) Neta, P. *J. Phys. Chem.* **1981**, *85*, 3678−3684.

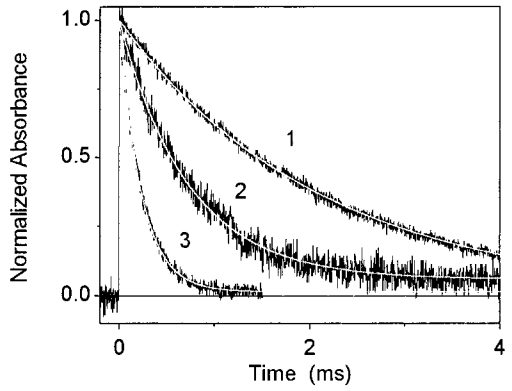

Figure 8. Decay of the transient absorptions at 460 nm following 532 nm photoexcitation of ZnTPPS.$^{4-}$ Conditions: 12.5 μM ZnTPPS $^{4-}$ in 20 mM acetate, pH 5.0. Trace 1: without additives; trace 2: plus 2 μM DHP vesicles and 42 μM TPP$^+$; trace 3: plus 1.4 μM TPP$^+$ without vesicles. Solid lines are first-order decay curves with $\tau = 2.1$ ms (1), 0.72 ms (2), and 0.17 ms (3).

can be estimated from the equation, $\phi = \phi_{isc}\phi_1\phi_t$, where ϕ_{isc}, the yield of photoexcited ZnTPPS^{4-} that undergo intersystem crossing to the triplet state, is 0.86.[17] Typically, under conditions where $\phi = 0.25$ (Table 1), $\phi_1 \cong 0.3$. Consequently, $\phi_t \cong 1$, that is, transmembrane electron transport occurs with nearly unitary efficiency. The increase in overall quantum yield for Co(bpy)$_3^{3+}$ reduction (ϕ) with increasing ionic strength (Table 1) can be attributed primarily to the corresponding increase in $(k_q)_v$.

Direct Photogeneration and Transmembrane Diffusion of TPP^o and TPTP^o. Photoexcited pyrylium and thiopyrylium ions are strongly oxidizing.[38] Reduction potentials for singlet-excited TPP$^+$ and TPTP$^+$ estimated from $E°$ (^{1}Pyr$^{+/o}$) = $E°$ (Pyr$^{+/o}$) + E_{00} are 2.66 and 2.91 V, respectively, where $E_{00} = 2.80$ and 2.88 eV is the singlet state energy for TPP$^+$ and TPTP$^+$.[39] Thus, singlet-excited pyrylium and thiopyrylium ions are thermodynamically capable of oxidizing acetate ion ($E° = 2.1$ V)[40] or water at pH 5.0 ($E° = 2.5$ V).[41] Nonetheless, we did not observe any fluorescence quenching of TPP$^+$ and TPTP$^+$ in acetonitrile containing 1 M H_2O or 20 mM acetate ions, suggesting that the first singlet excited states of TPP$^+$ and TPTP$^+$ are too short-lived to undergo bimolecular reactions at these acceptor concentrations.[42]

Pulsed laser excitation of TPP$^+$ and TPTP$^+$ at 355 nm in acetonitrile generated intermediates with lifetimes of ~20 μs and absorption maxima at 480 nm, which is characteristic of the excited triplet states for pyrylium and thiopyrylium ions.[43,44] These photoexcited states were quenched upon addition of water and sodium acetate, (Figure 9), yielding long-lived transients with absorption bands centered at 550 nm that are characteristic of TPP^o and TPTP^o radicals (Figure 10).[37,45] Rate constants determined for quenching of triplet-excited TPP$^+$ by H_2O and the acetate ion are 1 ($\pm$0.2) $\times$ 10^5 M^{-1} s^{-1} and 2.9 ($\pm$0.5) $\times$ 10^{10} M^{-1} s^{-1}, respectively; the corresponding values for triplet-excited TPTP$^+$ are 2.1 ($\pm$0.4) $\times$ 10^5 M^{-1} s^{-1} and 4.9 ($\pm$1) $\times$ 10^{10} M^{-1} s^{-1}.

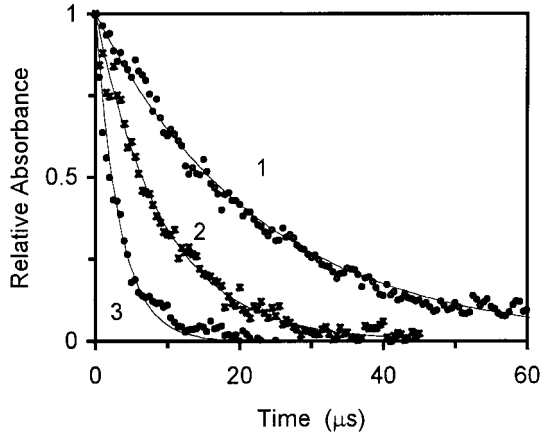

Figure 9. Decay of transient absorption at 480 nm following 355 nm photoexcitation of TPP$^+$ in acetonitrile. Conditions: [TPP$^+$] = 5 μM, E ~ 40 mJ/pulse. Trace 1: no additives; trace 2: plus 0.61 M H_2O; trace 3: plus 9 μM potassium acetate. Solid lines are first-order decay curves with $\tau = 23$ μs (1), 9.3 μs, (2) and 3.3 μs (3).

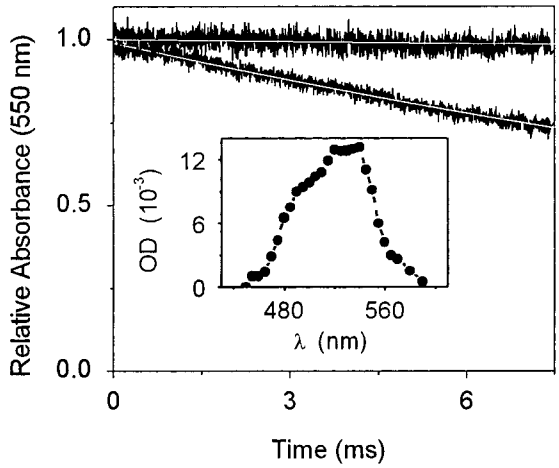

Figure 10. Decay of transient absorption at 550 nm following 355 nm photoexcitation of TPTP$^+$ in DHP vesicular suspensions. Conditions: [TPTP$^+$] = 5 μM, [DHP] = 2 mM, in 20 mM acetate, pH 5.0; $E \approx 150$ mJ/pulse. Upper trace: [Co(bpy)$_3^{3+}$] absent; lower trace:[Co(bpy)$_3^{3+}$] = 8 μM. Decay curves shown are averages of 10 individual runs. The transient absorption spectrum of the intermediate is shown in the inset.

Scheme 2

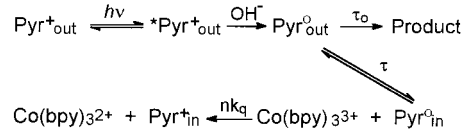

TPP^o and TPTP^o were also generated by direct pulsed laser excitation of TPP$^+$ and TPTP$^+$ in water and in vesicular suspensions. Their transmembrane diffusion rates were determined by measuring the rate of reduction of occluded Co(bpy)$_3^{3+}$, whose presence within the vesicles markedly increased the radical decay rates (Figure 10). The data were analyzed quantitatively according to Scheme 2 where k_q is the rate constant for reaction of the radical within a vesicle containing a single Co(bpy)$_3^{3+}$ ion, τ_o is the lifetime of Pyr^o when the DHP vesicles are not loaded with Co(bpy)$_3^{3+}$, and τ is the characteristic time for Pyr^o transmembrane diffusion. For vesicles containing nCo(bpy)$_3^{3+}$ ions, the rate constant for reaction is

(38) Miranda, M. A.; Garcia, H. *Chem. Rev.* **1994**, *94*, 1063−1089.
(39) Kuriyama, Y.; Arai, T.; Sakuragi, H.; Tokumaru, K. *Chem. Lett.* **1988**, 1193−1196.
(40) Dickinson, T.; Wynne-Jones, W. F. K. *Trans. Faraday Soc.* **1962**, *58*, 382−404.
(41) Kutal, C. *J. Chem. Ed.* **1983**, *60*, 882−887.
(42) Jayanthi, S. S.; Ramamurthy, P. *J. Phys. Chem A* **1997**, *101*, 2016−2022.
(43) Morlet-Savary, F.; Parret, S.; Fouassier, J. P.; Inomata, K.; Matsumo, T. *J. Chem. Soc., Faraday Trans.* **1998**, *94*, 745−752.
(44) Valat, P.; Tripathi, S.; Wintgens, V.; Kossanyi, J. *New J. Chem.* **1990**, *14*, 825−830.
(45) Jayanthi, S. S.; Ramamurthy, P. *J. Phys. Chem A.* **1998**, *102*, 511−518.

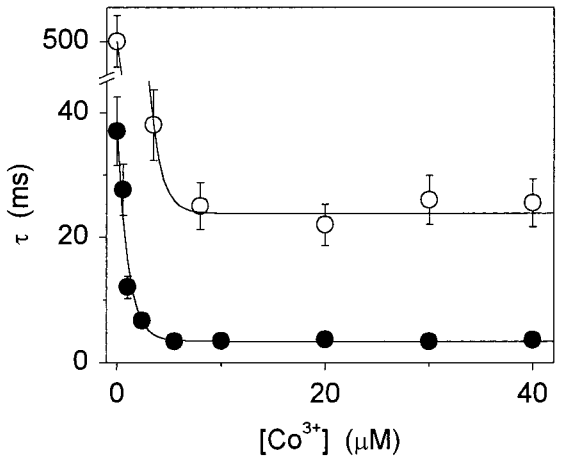

Figure 11. Dependencies of the characteristic times for TPP^o and $TPTP^o$ decay upon the concentration of occluded $Co(bpy)_3^{3+}$ in DHP vesicles. Conditions: ~2 μM DHP vesicles in 20 mM acetate, pH 5.0. Closed circles: TPP^o; open circles: $TPTP^o$; solid lines: best-fit curves obtained with equation S6 (Supporting Information) using $\tau_o = 37$ ms, $\tau = 3.8$ ms (TPP^o) and $\tau_o = 500$ ms, $\tau = 25$ ms ($TPTP^o$).

nk_q.[46] The characteristic decay time of the transient absorbances in the absence of $Co(bpy)_3^{3+}$ were determined to be $\tau_o = 37$ ms for TPP^o and $\tau_o \approx 500$ ms for $TPTP^o$. These values rapidly dropped in a concentration dependent manner at low [$Co(bpy)_3^{3+}$] to $\tau = 3.4$ ms and $\tau = 25$ ms, respectively, then became concentration-independent when [$Co(bpy)_3^{3+}$] $\geq 5-10$ μM (Figure 11). Rate equations obtained from the kinetic model presented in Scheme 2 are derived in the accompanying Supporting Information. From the characteristic times, assuming a bilayer width of 4 nm,[16] one obtains permeability coefficients for the radicals of $P_{TPP^o} = 1.0\ (\pm 0.03) \times 10^{-4}$ cm/s and $P_{TPTP^o} = 1.6\ (\pm 0.3) \times 10^{-5}$ cm/s.

Conclusions

The structural organization and dynamical properties of these assemblies are consistent with the simple reaction model depicted in Figure 1 which relies upon ring-opening hydrolysis and ring-closing dehydration of charged species to generate appropriate membrane-permeable neutral molecules. Specifically, transmembrane electron transfer is initiated by oxidative quenching of the $ZnTPPS^{4-}$ photosensitizer in the bulk phase by either the pyrylium (thiopyrylium) cation or its open ring hydrolysis product (Scheme 1). Subsequent transmembrane diffusion of the neutral pyrylium (thiopyrylium) radical and electron transfer to an electron acceptor regenerates the cation within the membrane. Ring-opening hydrolysis then generates the 1,5-diketone (thioglutaconic aldehyde) which can diffuse back across the membrane to the external phase. Subsequent ring-closing dehydration reforms the pyrylium (thiopyrylium) ion, closing the redox cycle. The redox mediator thereby functions as an electron$-OH^-$ antiporter whose cycling is electroneutral. The only mechanistic difference in the pathway involving oxidative quenching by the diketone (thioglutaconic aldehyde) is that, in this case (pathway b), electron transfer from the photosensitizer precedes, rather than follows (pathway a), the ring-closing reaction in the cycle. The pyrylium ions thereby function as both primary electron acceptor and cyclic transmembrane electron carrier in these systems. In principle, the pyrylium ions can also act as photosensitizers, obviating the need for additional chromophores. However, the particular compounds used underwent slow degradative photobleaching, which would limit their utility in applications requiring prolonged illumination.

Acknowledgment. This research is supported by the Division of Chemical Sciences, Office of Basic Energy Sciences, U.S. Department of Energy, under Grant DE-FG03-99ER14943.

Supporting Information Available: Figure S1, illustrating biphasic ring-opening hydrolysis of DHP vesicle-bound $TPTP^+$ at high dopant levels; Figure S2, illustrating the dependence of fluorescence spectra for DHP vesicle-bound $TPTP^+$ upon dopant levels; kinetic equations describing transmembrane diffusion of neutral pyrylium radicals (PDF). This information is available free of charge via the Internet at http://pubs.acs.org.

JA010017X

(46) Khairutdinov, R. F.; Serpone, N. *Prog. React. Kinet.* **1996**, *21*, 1−68.
(47) *Handbook of Chemistry and Physics*, 71st ed.; Lide, D. R., Ed.; CRC Press: Boca Raton, FL, 1990; pp (9-10)−(9-11).